Climate Change 2013: The Physical Science Basis

Summary for Policymakers

Drafting Authors: Lisa Alexander (Australia), Simon Allen (Switzerland), Nathaniel Bindoff (Australia), Francois-Marie Breon (France), John Church (Australia), Ulrich Cubasch (Germany), Seita Emori (Japan), Piers Forster (United Kingdom), Pierre Friedlingstein (United Kingdom), Nathan Gillett (Canada), Jonathan Gregory (United Kingdom), Dennis Hartmann (USA), Eystein Jansen (Norway), Ben Kirtman (USA), Reto Knutti (Switzerland), Krishna Kumar Kanikicharla (India), Peter Lemke (Germany), Jochem Marotzke (Germany), Valerie Masson-Delmotte (France), Gerald Meehl (USA), Igor Mokhov (Russia), Shilong Piao (China), Gian-Kasper Plattner (Switzerland), Qin Dahe (China), Venkatachalam Ramaswamy (USA), David Randall (USA), Monika Rhein (Germany), Maisa Rojas (Chile), Christopher Sabine (USA), Drew Shindell (USA), Thomas Stocker (Switzerland), Lynne Talley (USA), David Vaughan (United Kingdom), Shang-Ping Xie (USA)

Draft Contributing Authors (list to be updated): Olivier Boucher (France), Philippe Ciais (France), Peter Clark (USA), Matthew Collins (United Kingdom), Joey Comiso (USA), Gregory Flato (Canada), Jens Hesselbjerg Christensen (Denmark), Albert Klein Tank (Netherlands), Gunnar Myhre (Norway), Scott Power (Australia), Stephen Rintoul (Germany), Matilde Rusticucci (Argentina), Michael Schulz (Germany), Peter Stott (United Kingdom), Donald Wuebbles (USA)

Date of Draft: 5 October 2012

Notes: TSU Compiled Version

1. Introduction

The Working Group I contribution to the IPCC's Fifth Assessment Report presents new evidence of past and projected future climate change from many independent scientific studies ranging from observations of the climate system, paleoclimate archives, theoretical studies on climate processes and simulations using climate models.

The evidence that formed the basis for the IPCC Fourth Assessment Report (AR4)[1] has further strengthened. The physical science contributions to the recent Special Report on Managing the Risk of Extreme Events and Disasters to Advance Climate Change Adaptation (SREX)[2] serves as a basis of the current assessment regarding extreme weather and climate events.

A new set of emissions scenarios, the Representative Concentration Pathways (RCP) were used for the new climate model simulations carried out under the framework of the Coordinated Model Intercomparison Project 5 (CMIP5). The RCPs are mitigation scenarios which explore the effects of 21st century climate policies and thus differ from the no-climate policy scenarios used in previous assessment reports. The four RCPs span the range of year-2100 radiative forcing[3] values in the literature of 2.6 (RCP2.6) to 8.5 W m^{-2} (RCP8.5).

The degree of certainty in key findings in this assessment is expressed as a qualitative level of confidence and, when possible, probabilistically[4].

The basis for substantive paragraphs in this Summary for Policymakers can be found in the chapter sections specified in curly brackets.

2. Observation of Changes in the Climate System

Widespread changes in the atmosphere are observed across spatial and temporal scales. Strong evidence has emerged that the physical and biogeochemical state of the oceans has changed during the past forty years. Important parts of the cryosphere, in particular the extent and volume of snow and ice, have changed over the latter half of the 20th century. Paleoclimate archives provide quantitative information on the range of naturally driven changes in the climate system on time scales from centuries to millions of years.

AR4 concluded that warming of the climate system is unequivocal. New observations, longer data sets, and more paleoclimate information give further support for this conclusion. Confidence is stronger that many changes, that are observed consistently across components of the climate system, are significant, unusual or unprecedented on time scales of decades to many hundreds of thousands of years.

[1] IPCC, 2007: *Climate Change 2007: The Physical Science Basis*. Contribution of Working Group I to the Fourth Assessment Report of the Intergovernmental Panel on Climate Change [Solomon, S., D. Qin, M. Manning, Z. Chen, M. Marquis, K.B. Averyt, M. Tignor and H.L. Miller (eds.)]. Cambridge University Press, Cambridge, United Kingdom and New York, NY, USA, 996 pp.

[2] IPCC, 2012: *Managing the Risks of Extreme Events and Disasters to Advance Climate Change Adaptation*. A Special Report of Working Groups I and II of the Intergovernmental Panel on Climate Change [Field, C.B., V. Barros, T.F. Stocker, D. Qin, D.J. Dokken, K.L. Ebi, M.D. Mastrandrea, K.J. Mach, G.-K. Plattner, S.K. Allen, M. Tignor, and P.M. Midgley (eds.)]. Cambridge University Press, Cambridge, UK, and New York, NY, USA, 582 pp.

[3] Radiative Forcing (RF) is defined as the change in net irradiance at the tropopause since 1750 after allowing for stratospheric temperatures to readjust to radiative equilibrium, while holding surface and tropospheric temperatures and state variables fixed at the unperturbed values. Positive forcing tends to warm the surface while negative forcing tends to cool it. In this report, radiative forcing values are expressed in watts per square metre (W m^{-2}). (see Glossary)

[4] Mastrandrea, M.D., C.B. Field, T.F. Stocker, O. Edenhofer, K.L. Ebi, D.J. Frame, H. Held, E. Kriegler, K.J. Mach, P.R. Matschoss, G.-K. Plattner, G.W. Yohe, and F.W. Zwiers, 2010: *Guidance Note for Lead Authors of the IPCC Fifth Assessment Report on Consistent Treatment of Uncertainties*. Intergovernmental Panel on Climate Change (IPCC).

Atmosphere Observations

Widespread warming is observed from the surface of the Earth throughout the troposphere and cooling is identified in the stratosphere. Globally averaged near surface temperatures have increased since the beginning of the 20th century and the warming has been particularly marked since the 1970s. Each of the last three decades has been significantly warmer than all preceding decades since 1850. {2.4}

[INSERT FIGURE SPM.1 HERE]
Figure SPM.1: Multiple observed indicators of a changing global climate. Each line represents an independently derived estimate of change in various large-scale quantities from the atmosphere, the cryosphere, the land, and the ocean. In panels where individual datasets overlap, the datasets have been normalized to a common period of record. Anomalies are relative to the mean of 1981–2000 (panels a and b), 1971–2000 (panel c), 1961–1990 (panels e and f), and the year 1971 (panel h). Panel c provides the 13-year running mean of the March-April Snow Cover Extent (SCE) anomaly for the full observational record, and June SCE (x's) for the satellite period only. Full details of the datasets shown here are provided in the Supplementary Material to Chapters 2 and Chapter 4. Where available, uncertainties in the observations are indicated by a shaded range. {Figure 2.15, Figure 2.19, Figure 2.24, Figure 3.2, Figure 3.13, Figure 4.3, Figure 4.19}.

- The global combined land and ocean temperature data show an increase of about 0.8°C over the period 1901–2010 and about 0.5°C over the period 1979–2010 when described by a linear trend. The warming from 1886–1905 (early-industrial) to 1986–2005 is 0.66 [0.60 to 0.72] °C[5] (see Figure SPM.1). The warming since 1901 is generally greater over land than oceans and greater in mid-to-high latitude regions. {2.4.3}

- It is *virtually certain* that globally the troposphere has warmed and the lower stratosphere has cooled since the mid 20th century (see Figure SPM.1). There is at best *medium confidence* in the rates of these changes and their vertical structure. {2.4.4, Table 2.8}

- *Confidence* in global precipitation change over land is *low* prior to 1950 and *medium* afterwards because of incomplete data coverage. Precipitation data indicates little change in the global mean since 1900, which is a revision from previous assessments. {2.5.1, Figure 2.28}

- The mid-latitudes and higher latitudes of the northern hemisphere show an overall increase in precipitation from 1900–2010, however *confidence* is *low* because of much uncertainty in the data records for the early 20th century. Insufficient evidence exists to define a long-term temporal change of precipitation in the mid-latitudes of the southern hemisphere. Precipitation in the tropics has *likely* increased over the last decade, reversing the drying trend that occurred from the mid-1970s to mid-1990s. {2.5.1, Figure 2.28}

- It is *likely* that, in a zonal mean sense, large-scale atmospheric circulation features have moved poleward: since the 1970s the tropical belt has widened, storm tracks and jet streams have shifted poleward, and the polar vortex has contracted. {2.7}.

Changes in many extreme weather and climate events have been observed, but the level of confidence in these changes varies widely depending on type of extreme and regions considered. Overall the most robust global changes are seen in measures of temperature {FAQ 2.2, 2.6} (see Table SPM.1).

[5] In the WGI contribution to the AR5, uncertainty is quantified using 90% uncertainty intervals unless otherwise stated. The 90% uncertainty interval, reported in square brackets, is expected to have a 90% likelihood of covering the value that is being estimated. The upper endpoint of the uncertainty interval has a 95% likelihood of exceeding the value that is being estimated and the lower endpoint has a 95% likelihood of being less than that value. A best estimate of that value is also given where available. Uncertainty intervals are not necessarily symmetric about the corresponding best estimate.

- It is *very likely* that the overall number of cold days and nights has decreased and the overall number of warm days and nights has increased on the global scale between 1951 and 2010. There is *medium confidence* that the length of warm spells, including heat waves, has increased globally since the middle of the 20th century (see Table SPM.1). {2.6.1}

- There have been statistically significant trends in the number of heavy precipitation events in some regions. It is *likely* that the number of heavy precipitation events has increased in more regions than it has decreased since 1950 (see Table SPM.1). {2.6.2}

- There is *low confidence* in observed large-scale trends in drought, due to lack of direct observations, dependencies of inferred trends on the index choice, and geographical inconsistencies in the trends (see Table SPM.1). {2.6.2}

- Tropical cyclone data provides *low confidence* that any reported long-term changes are robust, after accounting for past changes in observing capabilities. This is a revision from previous IPCC Assessments Reports, but consistent with the SREX. Over the satellite era, increases in the intensity of the strongest storms in the Atlantic appear robust (see Table SPM.1). {2.6.3}

[INSERT TABLE SPM.1 HERE]
Table SPM.1: Recent trends, assessment of human influence on the trend, and projections for extreme weather and climate events for which there is an observed late-20th century trend. Bold indicates a revised assessment since AR4 (2007), (*) indicates a revised assessment from the SREX (2012) and (#) indicates that an assessment was not provided by either AR4 or SREX. {TS TFE9.1, 2.6, 11.3.2, 12.4.3, 12.4.4, 12.4.5}

Ocean Observations

Based on independent observational systems and datasets, and their agreement, it is *virtually certain* that the upper ocean has warmed since 1971, and that ocean warming dominates the change in the global energy content. {3.2.2, 3.2.3, Box 3.1, FAQ 3.1, Figure 3.1}

- Largest warming is found near the sea surface (>0.1°C per decade in the upper 75 m), decreasing to about 0.015°C per decade by 700 m, for the time period 1971 to 2010. It is *likely* that the deep ocean has warmed below 3000 m depth since the 1990s. The global ocean has warmed at a rate of <0.01°C per decade below 4000 m over this time interval. It is *very likely* that the Southern Ocean has warmed throughout the full ocean depth since the 1990s, at a rate of about 0.03°C per decade. {3.2, Figure 3.1, Figure 3.3}

- Warming of the ocean accounts for more than 90% of the extra energy stored by the Earth between 1971 and 2010. Upper ocean (0–700 m) heat content *very likely* increased at a rate between 74 [43 to 105] $\times 10^{12}$ W and 137 [120 to 154] $\times 10^{12}$ W for the relatively well-sampled 40 year period from 1971 to 2010. Warming has also been observed globally below 4000 m and below 1000 m in the Southern Ocean, in spite of sparse sampling (see Figure SPM.1). {3.2, Box 3.1, Figure 3.2, Figure 3.3}

- It is *very likely* that the mean regional pattern of sea surface salinity has been enhanced since the 1960s: saline surface waters in the evaporation-dominated mid-latitudes have become more saline, while the relatively fresh surface waters in rainfall-dominated tropical and polar regions have become fresher. {3.3.2, Figure 3.4, FAQ 3.3}

- Recent observations have strengthened evidence for variability in major ocean circulation systems on time scales from years to decades. It is *very likely* that the subtropical gyres in the North Pacific and South Pacific have expanded and strengthened since 1993. There is no evidence for decadal trends in the transports of the Atlantic Meridional Overturning Circulation (AMOC), and the Antarctic Circumpolar Current. {3.6, Figure 3.10, Figure 3.11}

Cryosphere Observations

More comprehensive and improved observations strengthen the evidence that the ice sheets are losing mass, glaciers are shrinking globally, sea ice cover is reducing in the Arctic, and snow cover is decreasing and permafrost is thawing in the Northern Hemisphere. Ice is being lost from many of the components of the cryosphere, although there are significant regional differences in the rates of loss. {4.2–4.6, Table 4.1}

- There is *very high confidence* that globally, glaciers continue to shrink and lose mass, but there is less agreement on the rates of mass loss. Recent estimates of global glacier mass loss based on independent methods range from 210 [145 to 275] Gt yr^{-1} to 371 [321 to 421] Gt yr^{-1}, based on different time windows since 2003. {4.3, Table 4.5}.

- There is *very high confidence* that the Greenland Ice Sheet has lost mass since the early 1990s, and that the rate of loss has increased. The average ice loss from Greenland was 123 [101 to 145] Gt yr^{-1} over the period 1993–2010, and 228 [174 to 282] Gt yr^{-1} in the period 2005–2010. {4.4.2}

- There is *high confidence* that the Antarctic Ice Sheet is currently losing mass. The average ice loss from Antarctica was 65 [32 to 98] Gt yr^{-1} over the period 1993–2010, and 112 [54 to 170] Gt yr^{-1} over the period 2005–2010. The largest ice losses from Antarctica have occurred on the northern Antarctic Peninsula and from the Amundsen Sea sector of West Antarctica. In the last two decades, East Antarctica is *likely* to have experienced a small gain in mass. {4.4.2, FAQ 4.2}

- The average decadal extent of Arctic sea ice has decreased in every season since satellite observations commenced in 1979. The overall decrease in sea ice extent over the period 1979–2011 has been 3.9 [3.7 to 4.1] % per decade with larger changes occurring in summer and autumn (see Figure SPM.1). There is robust evidence of a decline in ice thickness, and in ice volume. The overall mean winter thickness has about halved between 1980 and 2009. {4.2.2}

- Observations of Antarctic sea ice extent show a small but significant increase by 1.4 [1.2 to 1.6] % per decade between 1979 and 2011. {4.2.3}

- Both satellite and in-situ observations show significant reductions in the Northern Hemisphere snow cover extent over the past 90 years, with most reduction occurring in the 1980s (see Figure SPM.1). Snow cover decreased most in spring when the average extent decreased by around 8% over the period 1970–2010 compared with the period 1922–1970. {4.5.2, Figure 4.19, Figure 4.20}

- There is *high confidence* that permafrost temperatures have increased by up to 3°C over major permafrost regions of the Northern Hemisphere during the past three decades in response to increased air temperature and changing snow cover. {4.6.2}

Sea Level Observations

It is unequivocal that global mean sea level is rising as is evident from tide gauge records and satellite data (see Figure SPM.1).

- It is *virtually certain* that over the 20th century the mean rate of increase was between 1.4 to 2.0 mm yr^{1}, and between 2.7 and 3.7 mm yr^{-1} since 1993. It is *likely* that rates of increase were similar to the latter between 1930 and 1950. {3.7.2, 3.7.3, Table 3.1, Figure 3.12, Figure 3.13}

- It is *likely* that extreme sea levels have increased since 1970, and this is mainly caused by rising mean sea level. {3.7.5}

Observation of Carbon and Other Biogeochemical Quantities

More than half of the total carbon emitted by human activities has been taken up by the ocean and the land since 1750. The remainder has caused an increase in the atmospheric CO_2 concentration by over 40% since 1750, and by about 10% since 1990. {6.3, Table 6.1, Figure 6.8}

- CO_2 emissions from fossil fuel combustion and cement production estimated from energy statistics have released 365 [335 to 395] PgC[6] to the atmosphere, while deforestation and other land use change are estimated to have released 180 [100 to 260] PgC since 1750. Of these 545 [460 to 630] PgC, only 240 [230 to 250] PgC have accumulated in the atmosphere and increased the atmospheric CO_2 concentration from 278 [273 to 283] ppm[7] in 1750 to 390 ppm in 2011 (see Figure SPM.2). {6.3, Table 6.1, Figure 6.8}

[INSERT FIGURE SPM.2 HERE]
Figure SPM.2: Multiple observed indicators of a changing global carbon cycle. Measurements of atmospheric concentrations of carbon dioxide (CO_2) are from Mauna Loa and South Pole since 1958. Measurements of partial pressure of CO_2 at the ocean surface are shown from three stations from the Atlantic and the Pacific Oceans, along with the measurement of in situ pH, a measure of the acidity of ocean water. These stations are the Hawaii Ocean Time-series (HOT) from the station ALOHA, the Bermuda Atlantic Time-series Study (BATS), and the European Station for Time series in the Ocean (ESTOC). Full details of the datasets shown here are provided in the underlying report. {Figure 2.1, Figure 3.17}.

- It is *virtually certain* that the ocean is taking up anthropogenic carbon dioxide from the atmosphere. There is *very high confidence* that the global ocean content of anthropogenic carbon increased from 1994 to 2010. Estimates range from 93–137 PgC in 1994 to 155 [125 to 185] PgC in 2010. {3.8.1, Figure 3.15, Figure 3.16}

- There is *very high confidence* that oceanic uptake of anthropogenic CO_2 has resulted in gradual acidification of seawater evidenced by a decreasing pH in surface waters at a rate of between 0.015 and 0.024 per decade since the early 1980s (see Figure SPM.2). {3.8.2, Table 3.2, Box 3.2, FAQ 3.2, Figure 3.17, Figure 3.18}

- Natural terrestrial ecosystems not affected by land use change are estimated to have accumulated 150 [60 to 140] PgC since 1750. {6.3, Table 6.1, Figure 6.8}

Long-Term Perspective from Paleoclimatic Records

Analyses of a number of independent paleoclimatic archives provide a multi-century perspective of Northern Hemisphere temperature and indicate that 1981–2010 was *very likely* the warmest 30-year period of the last 800 years. {5.3.5}

- There is *medium confidence* that in the Northern Hemisphere 1981–2010 was the warmest 30-year period of the last 1300 years. There is *high confidence* that the Medieval Climate Anomaly, about 900 to 1400 CE, shows inconsistent temperature changes across seasons and regions, in contrast to the widespread temperature increase of the late 20st century. {5.3.5, 5.5.1}

[6] 1 Petagram of carbon = 1 PgC = 10^{15} grams of carbon = 1 Gigatonne of carbon = 1 GtC. This corresponds to 3.67 $GtCO_2$.
[7] ppm (parts per million) or ppb (parts per billion, 1 billion = 1,000 million) is the ratio of the number of greenhouse gas molecules to the total number of molecules of dry air. For example, 300 ppm means 300 molecules of a greenhouse gas per million molecules of dry air.

- There is *medium confidence* that the current near-global recession of glacier length is unusual in the context of the last two millennia, consistent with reconstructed surface-temperature anomalies. There is *high confidence* that retreating glaciers are still larger now than in the early-to-mid Holocene in most regions, and that this is consistent with the astronomically driven trends of summer insolation and temperatures in both hemispheres. {5.5.3}.

- There is *medium confidence* that the modern sea ice loss and increase of sea surface temperatures in the Arctic are anomalous in the perspective of at least the last two millennia. Summer sea ice cover between 8,000 and 6,500 years before the present was reduced compared to late 20th century levels both in the Arctic Ocean and along East Greenland consistent with increased astronomically driven summer insolation in the Northern Hemisphere. {5.5.2}

- There is *high confidence* that during the last interglacial period, global mean sea level was between 6 and 10 m higher than present. There is *medium confidence* that the rate of current global mean sea level change is unusually high in the context of the past millennium. Paleo sea level data from many locations around the globe indicate centennial to millennial variations of *likely* less than 25 cm (*medium confidence*). Longer term trends of sea level change during the last few thousand years were about 10 times smaller than the trend during the 20th century. {3.7, 5.6, 13.2}

3. Drivers of Climate Change

Natural and anthropogenic drivers cause imbalances in the Earth's energy budget. The strongest anthropogenic drivers are changes in greenhouse gas concentrations and aerosols. These can now be quantified in more detail, but the uncertainties of the forcing associated with aerosols remain high.

Globally, CO_2 is the strongest driver of climate change compared to other changes in the atmospheric composition, and changes in surface conditions. Its relative contribution has further increased since the 1980s and by far outweighs the contributions from natural drivers. CO_2 concentrations and rates of increase are unprecedented in the last 800,000 years and at least 20,000 years, respectively. Other drivers also influence climate on global and particularly regional scales. {5.2.2, 8.3.2, 8.5.1, Figure 8.6, Figure 8.17}

- Multiple lines of evidence confirm that the long-lived greenhouse gases CO_2, CH_4, N_2O all have increased substantially since 1750. There is *very high confidence* that they now exceed by 30%, 125%, 8%, respectively, the range of variability recorded in ice core records during past 800,000 years, noting that ice cores typically produce values averaged over many years. {5.2.2, 6.3, Table 6.1, Figure 6.8}

- Since systematic measurements of CO_2 began in 1958 annual mean concentrations have constantly increased and are now 24% higher than at the start of the record (see Figure SPM.2). {6.3, Table 6.1, Figure 6.8}

- It is *virtually certain* that atmospheric concentrations of long-lived greenhouse gases further increased from 2005 to 2011. Annual increases in global mean CO_2 and N_2O mole fractions were at rates comparable to those observed over the previous decade. Atmospheric CH_4 began increasing again in 2007 after remaining nearly constant from 1999 to 2006. {2.2.1, Table 2.1}

[INSERT FIGURE SPM.3 HERE]
Figure SPM.3: Global average radiative forcing (RF) estimates and ranges for various drivers and three successive time periods; 1750–1950, 1750–1980, 1750–2011. The anthropogenic drivers are carbon dioxide (CO_2), other well-mixed greenhouse gases (CH_4, N_2O, and others), ozone, land use change, statospheric water vapour, and aerosols, with the sum of all contributions indicated. Assessed uncertainty ranges are given by black intervals. The RF of solar irradiance, a natural driver, is also estimated for the three time periods. {Figure 8.17}

There is consistent evidence from observations of a net energy uptake of the Earth System due to an imbalance in the energy budget. It is *virtually certain* that this is caused by human activities, primarily by the increase in CO_2 concentrations. There is *very high confidence* that natural forcing contributes only a small fraction to this imbalance (see Figure SPM.3). {8.4.1, 8.5.1, 8.5.2, Figure 8.13, Figure 8.14, Figure 8.17, Figure 8.19}

- The total anthropogenic RF has a best estimate of 2.40 [1.80 to 3.00] W m^{-2} (see Figure SPM.3) The estimate of total anthropogenic RF is 50% higher compared to previous assessments due primarily to a better understanding of aerosols which led to less negative estimates of aerosol RF, but also to continued growth in greenhouse gas RF. {8.5.1, Figure 8.17}

- The RF of well-mixed greenhouse gases is 2.83 [2.55 to 3.11] W m^{-2}. CO_2 alone contributes 1.82 [1.64 to 2.00] W m^{-2} and is *virtually certain* to be the strongest component causing a positive RF (see Figure SPM.3). {8.3.2, Figure 8.6}

- Short-lived greenhouse gases contribute substantially to RF. The total RF due to changes in ozone is 0.30 [0.10 to 0.50] W m^{-2}, with RF due to tropospheric ozone of 0.40 [0.20 to 0.60] W m^{-2} and due to stratospheric ozone of –0.10 [–0.25 to +0.05] W m^{-2} (see Figure SPM.3). {8.3.3, Figure 8.8}

- The total RF from aerosols is estimated to be –0.7 [–1.2 to –0.2] W m^{-2} (see Figure SPM.3). The uncertainty in the aerosol contribution dominates the overall net uncertainty in RF, but there is *high confidence* that aerosols have offset part of the forcing caused by the well-mixed greenhouse gases. {8.3.4, 8.5.1, Figure 8.17}

- The RF of stratospheric aerosols is well understood and can have a large impact on the climate for years to decades after volcanic eruptions. Several small eruptions have caused a RF of about –0.10 [–0.13 to –0.07] W m^{-2} during the 2000 to 2010 period. {8.4.2, Figure 8.15, Figure 8.18}

- Persistent contrails from aviation contribute a RF of +0.02 [+0.01 to +0.03] W m^{-2}. This forcing can be much larger regionally but is *very unlikely* to produce observable regional effects on either the mean or diurnal range of surface temperature. {7.2.5}

- Secular trends of total solar irradiance before the start of satellite observations rely on a number of indirect proxies with a best RF estimate of +0.04 [–0.01 to +0.09] W m^{-2} since 1750 (see Figure SPM.3). Satellite observations of total solar irradiance changes since 1978 spanning three solar cycle minima show a change in RF of –0.04 [–0.06 to –0.02] W m^{-2} over the last three decades. This RF estimate is substantially lower than previous estimates due to data of the latest solar cycle and inconsistencies in how solar RF has been estimated in earlier assessments. {8.4.1, Figure 8.13, Figure 8.14}

- Cosmic rays enhance aerosol nucleation and cloud condensation nuclei production in the free troposphere, but there is *high confidence* that the effect is too weak to have any significant climatic influence during a solar cycle or over the last century. No robust association between changes in cosmic rays and cloudiness has been identified. {7.3, 7.4.5}

4. Understanding the Climate System and its Recent Changes

Understanding of the climate system is based on the quantitative combination of observations, theoretical studies of feedback processes, and model simulations. More detailed observations and improved climate models now enable the attribution of detected changes to the increases in greenhouse gas concentrations in a wider range of climate system components.

Evaluation of Climate Models

Development of climate models has resulted in more realism in the representation of many quantities and aspects of the climate system, including large scale precipitation, Arctic sea ice, ocean heat content, extreme events, and the climate effects of stratospheric ozone. {9.4.1, 9.4.2, 9.4.3, 9.5.4, Figure 9.6, Figure 9.17}

- There is *very high confidence* that coupled climate models provide realistic responses to external forcing. This is evident from simulations of the surface temperature on continental and larger scales, and the global-scale surface temperature increase over the historical period, especially the last fifty years. {9.4.1, Box 9.1, Figure 9.2, Figure 9.8, 10.2, 11.3, 12.2}

- The simulation of large-scale patterns of precipitation has improved since the AR4, but there is only *medium confidence* that models simulate realistic amounts of precipitation increases in wet areas and precipitation decreases in dry areas on large spatial scales during the past 50 years, based on high agreement among models but only limited evidence that this has been detected in observed trends. {9.4.1,10.3.2, 11.4.2, 12.4.5}

- There is *very high confidence* that climate models realistically simulate the annual cycle of Arctic sea-ice extent, and there is *high confidence* that they realistically simulate the trend in Arctic sea ice extent over the past decades. {9.4.3}.

- There is *high confidence* that many models simulate realistically the observed trend in ocean heat content. {9.4.2, Figure 9.17, Box 13.1}.

- The combination of information from ocean warming and changes in glacier and ice sheet volume and land water storage is now, within the uncertainties, in quantitative agreement with observations of total sea level rise for the last four decades. This is a significant advance since the AR4 and strengthens the confidence in the physical understanding and modelling of the causes of past global mean sea level change. {4.3.1, 4.4.2, 13.3.6, Table 13.1, Figure 13.4, Figure 13.5, FAQ 3.1}

- There is *high confidence* that the global distribution of temperature extremes is represented well by models. The observed warming trend of temperature extremes in the second half of the 20th century is well simulated. There is *medium confidence* that CMIP5 models tend to simulate more intense and thus more realistic precipitation extremes than CMIP3 models. {9.5.4}

- Since AR4, many climate models have been extended with biogeochemical cycles into Earth System Models (ESMs). There is *high confidence* that most ESMs produce global land and ocean carbon sinks over the latter part of the 20th century that are consistent with the range of observational estimates. {9.4}

Climate Processes and Feedbacks

Various feedbacks associated with water vapour can now be quantified, and together they are assessed to be *very likely* positive and therefore to amplify climate changes. The net radiative feedback due to all cloud types is *likely* positive. {7.2.4, Figures 7.8–7.10}

- The net "clear-sky" feedback from water vapour and lapse rate changes together is *very likely* positive and estimated at +1.09 [0.91 to 1.27] W m^{-2} K^{-1}, and the cloud feedback is *very likely* in the range of −0.2 to 1.4 W m^{-2} K^{-1}. {7.2.4, Figures 7.8–7.10}

- A limited number of modelling studies have quantified the aerosol-climate feedback as 0.0 [–0.2 to +0.2] W m^{-2} K^{-1} although with *low confidence*. {7.3.4, 7.5.2}

- Paleoclimate reconstructions and modelling indicate that there is a positive feedback between climate and the carbon cycle on century to millennial time scales, i.e., when climate warms land and ocean carbon storage are reduced. {6.3.2, 6.4}

Detection and Attribution of Climate Change

It is *extremely likely* that human activities have caused more than half of the observed increase in global average surface temperature since the 1950s. There is *high confidence* that this has caused large-scale changes in the ocean, in the cryosphere, and in sea level in the second half of the 20th century. Some extreme events have changed as a result of anthropogenic influence. {10.3–10.6}

[INSERT FIGURE SPM.4 HERE]
Figure SPM.4: Comparison of observed and simulated climate change based on four large-scale indicators in the atmosphere, cryosphere and the ocean. Indicators are time series of continental land surface air temperatures (1850–2010, yellow padded panels), zonal mean precipitation in latitude bands (1950–2010, green padded panels), Arctic and Antarctic sea ice (1950–2010, white padded panels), and ocean heat uptake in the major ocean basins (1950–2010, blue padded panels). Global mean changes are also given. In all panels, black/grey curves indicate observation-based estimates, blue curves and bands are multi-model mean and ensemble ranges based on simulations forced by natural drivers only, and red curves and bands are for simulations forced by natural and anthropogenic drivers. The bands indicate the 5 to 95% for temperature, and one standard deviation for precipitation, sea ice, and ocean heat content. Model results are based on the ensemble of CMIP5. For sea ice extent the seven CMIP5 models are considered that matched the mean minimum and seasonality with less than 20% error compared with observations. Full details are provided in the Appendix of Chapter 10. {Figure 10.15, 10.20}

- The greenhouse gas contribution to the warming from 1951–2010 is in the range between 0.6 and 1.4°C. This is *very likely* greater than the total observed warming of approximately 0.6°C over the same period. {10.3.1}

- Over every continent except Antarctica, anthropogenic influence has *likely* made a substantial contribution to surface temperature increases since the mid-20th century (see Figure SPM.4). {10.3.1}

- It is *very likely* that early 20th century warming is due in part to external forcing, including greenhouse gas concentrations, tropospheric aerosols, and solar variations. Climate model simulations that include only natural forcings (volcanic eruptions and solar variations) can explain a substantial part of the pre-industrial inter-decadal temperature variability since 1400 but fail to explain more recent warming since 1950 (see Figure SPM.4). {10.3.1, 10.7.2}

- It is *very likely* that more than half of the ocean warming observed since the 1970s is caused by external forcing, mainly due to a combination of both anthropogenic forcing and volcanic eruptions (see Figure SPM.4). It is *extremely likely* that this warming has resulted in global mean sea level rise due to thermal expansion during this period. {10.4.1, 10.4.3}

New observations and their combination with climate model simulations now permit the attribution of some changes in the water cycle since 1950 to anthropogenic influences. Taken together, these patterns are consistent with an intensified global water cycle. {10.3.2}

- There is *medium confidence* for anthropogenic contributions to an increase in atmospheric moisture content and tropospheric specific humidity, and to changes in zonal precipitation patterns over land with reductions in low latitudes and increases in northern hemisphere mid to high latitudes since 1950 (see Figure SPM.4).

- It is *likely* that observed changes in ocean surface and sub-surface salinity are due in part to the changes in the water cycle caused by anthropogenic increases in greenhouse gases. {10.3.2}

- It is *likely* that anthropogenic forcings have contributed to Arctic sea ice retreat since 1950. There is *medium confidence* that the observed small net increase in Antarctic sea ice extent is consistent with internal variability (see Figure SPM.4). Human influences are the *likely* cause for a substantial reduction in glaciers since the 1960s (*high confidence*), and reductions in snow cover and permafrost since the 1970s (*medium confidence*). {10.5.1, 10.5.2}

- It is *likely* that anthropogenic forcings have contributed to the increased surface melt of Greenland since 2000. There is only *low confidence* of a human contribution to the observed loss of Antarctic ice sheet mass since 1990 due to limited scientific understanding of the processes involved. {10.5.1, 10.5.2}

- It is *very likely* that anthropogenic forcing has contributed to the observed changes in daily temperature extremes since the mid-20th century. It is *likely* that human influence has substantially increased the probability of some observed heatwaves. There is *medium confidence* that anthropogenic forcing has contributed to an increase in the frequency of heavy precipitation events over the second half of the 20th century over land regions with sufficient observational coverage. {10.6}

- Consistent with SREX, there is *low confidence* in attribution of changes in tropical cyclone activity to human influence due to insufficient observational evidence and low level of agreement between studies. {10.6}.

Key Metrics Characterizing Anthropogenic Climate Change

- Equilibrium climate sensitivity is *likely* in the range 2°C–4.5°C, and *very likely* above 1.5°C. The most likely value is near 3°C. Equilibrium climate sensitivity greater than about 6°C–7°C is *very unlikely*. {Box 12.2}

- The total amount of anthropogenic emissions of long-lived greenhouse gases largely determines the warming in the 21st century. The global mean warming per 1000 PgC is *very likely* between 0.8°C–3°C. {12.5.4}

- Different metrics can be used to quantify the contributions to climate change of emissions of different substances, and of emissions from regions/countries or sources/sectors. No single metric can accurately compare all consequences of different emissions. The choice of metric therefore depends strongly on the particular impact being investigated, and on the context in which it is applied. {8.7.1}

5. Projections of Global and Regional Climate Change

Projections of changes in the climate system are based on simulations using a hierarchy of climate models ranging from simple climate models, to models of intermediate complexity, and comprehensive Earth System Models. These models simulate changes based on a variety of scenarios of natural and anthropogenic forcings.

- Projected climate change for the RCPs is similar to AR4 when accounting for scenario differences. Uncertainties for the high RCPs are lower because carbon cycle uncertainties are not considered. Simulated patterns of climate change in the CMIP5 models are very similar to CMIP3, despite substantially increased model complexity, thus increasing the confidence in projections. {11.3.6, 12.3, 12.4, 12.4.9}

- Projections of near-term climate change depend little on differences in greenhouse gas and aerosol emissions within the range of the RCP scenarios. These scenarios assume that there are no major volcanic eruptions and that anthropogenic aerosol emissions are rapidly reduced during the near term. {11.3.2, 11.3.5}

Projections of many quantities on the near-term time horizon already provide an indication of changes later in the 21st century. The confidence in these projections is often assessed to be lower for the near-term than for later in the 21st century. {11.3.1, 11.3.6, Box 11.1, FAQ 11.1}

Near-Term Projections: Atmosphere

- The global mean surface air temperature change for the period 2016–2035 relative to the reference period of 1986–2005[8], will *likely* be in the range 0.4°C–1.0°C (*medium confidence*) (see Figure SPM.5). There is robust evidence that collectively the RCPs represent the low end of future emissions scenarios for aerosols and other short-lived reactive gases. Therefore, it is *more likely than not* that actual warming will be closer to the lower bound of 0.4°C than the upper bound of 1.0°C (*medium confidence)*. {11.3.2, Figure 11.33}

- A future volcanic eruption similar in size to the 1991 eruption of Mount Pinatubo would cause a rapid drop in global mean surface air temperature of several tenths of 1°C in the following year, with recovery over the next few years. Possible future reductions in solar irradiance would reduce global mean surface air temperature, but such cooling is *unlikely* to exceed –0.1°C by 2050 (*medium confidence*). {11.3.6}

- It is *more likely than not* that over the next few decades there will be increases in mean precipitation in regions and seasons that are relatively wet during 1986–2005, and decreases in regions and seasons that are relatively dry during 1986-2005. However, it is *likely* that these changes from 1986–2005 will only be significant, relative to natural internal variability, on the largest spatial scales, e.g., zonal and global means (see Figure SPM.5). {11.3.2, Figure 11.16}

- Over the next few decades increases in near-surface specific humidity are *very likely*. Models project increases in evaporation in most regions. There is *low confidence* in projected changes in soil moisture and surface run off. Natural internal variability will continue to have a major influence on all aspects of the water cycle. {11.3.2, Figure 11.18}

- It is *very likely* that in the next decades the frequency of warm days and warm nights will increase, while the frequency of cold days and cold nights will decrease at the global scale. Models also project increases in the duration, intensity and spatial extent of heat-waves and warm spells for the near term. {11.3.2, Figure 11.22, Figure 11.23}

- In the near term, it is *likely* that the frequency and intensity of heavy precipitation events will increase at the global scale and at high latitudes. Regional-scale changes are strongly affected by natural variability and also depend upon the future aerosol emissions, volcanic forcing and land use changes.{11.3.2, Figure 11.22, Figure 11.23}

Near-Term Projections: Ocean

- It is *virtually certain* that globally-averaged surface and upper ocean (top 700 m) temperatures averaged over 2016–2035 will be warmer than those averaged over 1986–2005. {11.3.3}

[8] In this WGI Summary for Policymakers, projections of future climate change are generally compared to the standard reference period of 1986–2005, unless otherwise stated.

- Overall, it is *likely* that there will be some decline in the AMOC by 2050. However, the rate and magnitude of weakening is very uncertain, and decades when this circulation increases are also to be expected {11.3.3}.

Near-Term Projections: Cryosphere

- It is *very likely* that there will be continued loss of sea ice extent in the Arctic, decreases of snow cover, and reductions of permafrost at high latitudes of the Northern Hemisphere by 2016–2035. Using RCP4.5, Arctic sea ice area is projected to decrease by 28% for September and 6% for February; Northern Hemisphere snow cover area is projected to decrease by 4.0 [2.1 to 5.9] % (one standard deviation) for a March-April average; annual mean near-surface permafrost is projected to decrease by 18%. {11.3.4}

[INSERT FIGURE SPM.5 HERE]
Figure SPM.5: CMIP5 multi-model simulated time series. Panel (a) provides the radiative forcing reconstructed for the historical time period and projected for the future. Other panels provide mean changes (relative to 1986–2005) of (b), global annual mean surface air temperature, (c), global annual mean precipitation, (d), Northern Hemisphere sea-ice extent anomaly in September, and (e), global mean ocean surface pH from CMIP5 climate model simulations from 1850 to 2100. Projections are shown for emissions scenarios RCP2.6 (blue) and RCP8.5 (red) for the multi-model mean (solid lines) and ±1 standard deviation across the distribution of individual model simulations (shading). Black (grey shading) is the modelled historical evolution using historical reconstructed forcings. For pH, a subset of the CMIP5 models is chosen which simulate the global carbon cycle and which are driven by prescribed atmospheric CO_2 concentrations. The number of CMIP5 models to calculate the multi-model mean is indicated for each time period/scenario. {Figure 12.5, Figure 12.28, Figure 6.28}

[INSERT FIGURE SPM.6 HERE]
Figure SPM.6: Maps of multi-model results in 2081–2100 (relative to 1986–2005) of (a), surface air temperature change, (b), average percent change in mean precipitation, (c), Northern Hemisphere sea ice concentration, and (d) change in global ocean surface pH. The two emissions scenarios RCP2.6, and RCP8.5 are considered. The number of CMIP5 models to calculate the multi-model mean is indicated in the upper right corner of each panel. The pink lines in panels (c) show the observed 15% sea ice concentration limits averaged over 1986–2005 for comparison. {Figure 12.11, Figure 12.22, Figure 12.29, Figure 6.28}. [PLACEDHOLDER FOR SECOND ORDER DRAFT: Information on robustness and model agreement to be considered.]

[INSERT TABLE SPM.2 HERE]
Table SPM.2: Projected change in global average surface air temperature (SAT) and sea level rise (SLR) for three time horizons during the 21st century. {Table 12.2, Table 13.5, 12.4.1, 11.3.2}

Long-Term Projections: Temperature

By mid-21st century, the rate of global warming begins to be more strongly dependent on the scenario. For RCP4.5, 6.0 and 8.5, global mean surface air temperatures are projected to at least *likely* exceed 2°C warming with respect to preindustrial by 2100, and about *as likely as not* to be above 2°C warming for RCP2.6 (see Figure SPM.5). {12.3.1, 12.4.1, Figure 12.2, Figure 12.5}

- Global-mean surface temperatures for 2081–2100 (relative to 1986–2005) for the CO_2 concentration driven RCPs will *likely* be in the 5–95% range of the CMIP5 climate models, i.e., 0.2°C–1.8°C (RCP2.6), 1.0°C–2.6°C (RCP4.5), 1.3°C–3.2°C (RCP6.0), 2.6°C–4.8°C (RCP8.5) (see Figure SPM.5, Table SPM.2). {8.5.3, Figure 8.20, Figure 8.21, 12.4.1, Figure 12.8}

- There is *very high confidence* that future changes in global land surface air temperature will exceed changes in global average ocean-area surface air temperature by a factor of 1.5 [1.3 to 1.7] (one standard deviation). There is *very high confidence* that the Arctic region will warm most rapidly (see Figure SPM.6). {12.4.3}

- It is *virtually certain* that, in most places, there will be more hot and fewer cold temperature extremes as global temperature increases. These changes are expected for events defined as extremes on both daily and seasonal time scales. Although increases in the frequency, duration and magnitude of hot extremes are expected, occasional cold winter extremes will continue to occur. {12.4.3}

- Under RCP8.5 it is *likely* that, in most regions, what is currently a 20-year maximum temperature event will at least double its frequency, but in many regions becoming 10 to 20 times more frequent, i.e., a 2-year to annual event, and that what is currently a 20-year minimum temperature event will become exceedingly rare by the end of the 21st century. {12.4.3}

Long-Term Projections: Atmospheric Circulation

- There is generally *low confidence* in basin-scale projections of trends in tropical cyclone frequency and intensity to the mid-21st century. Projections for the end of the 21st century indicate that it is *likely* that the global frequency of tropical cyclones will either decrease or remain essentially unchanged, concurrent with a *likely* increase in both global mean tropical cyclone maximum wind speed and rainfall rates. The frequency of the most intense tropical cyclones is projected to *more likely than not* increase substantially in some basins {11.3.2, Box 14.2}.

- It is *unlikely* that the global number of extra-tropical cyclones will decrease by more than a few percent due to global warming. {12.4.4}

Long-Term Projections: Water Cycle

Changes in precipitation in a warming world will not be uniform. The high latitudes are *very likely* to experience larger amounts of precipitation. Many regions in the mid-latitudes that are arid and semi-arid will *likely* experience less precipitation, while those that are moist will *likely* receive more precipitation. While there is *high confidence* in patterns of these changes, there is only *low confidence* in the magnitude (see Figure SPM.6). {12.4.5}

- It is *virtually certain* that global precipitation will increase with global mean surface temperature (see Figure SPM.5). It is *likely* that the rate of increase of precipitation with temperature will be in the range 1–3% K^{-1}, for scenarios other than RCP2.6. For RCP2.6 the range of sensitivities in the CMIP5 models is 0.5–4.0% K^{-1} at the end of the 21st century. {12.4.1, Figure 12.6}

- Regional to global-scale projections of soil moisture and drought remain relatively uncertain compared to other aspects of the hydrological cycle. Surface drying in the Mediterranean, southwestern North America and southern African regions is *likely* when global temperatures increase. {12.4.5}

- The frequency distribution of precipitation events is projected to *very likely* undergo changes as global temperatures increase. For short-duration events, a shift to more intense individual storms and fewer weak storms is *likely*. In moist and some arid and semi-arid regions, extreme precipitation events will *very likely* be more intense and more frequent. {12.4.5}

Long-Term Projections: Climate Phenomena

Climate phenomena exhibit large natural variations both in amplitude and spatial patterns. While they are increasingly well simulated by climate models, there still remain uncertainties in the physical understanding. This results in overall *low confidence* in projections in many aspects of these climate phenomena, although some projections are assessed to be robust. {9.5.3, 14.2–14.6}

- In high emission scenarios, global monsoon area and global monsoon total precipitation are *very likely* to increase by the end of the 21st century. Monsoon onset dates are *likely* to become earlier or not to change much, and the monsoon retreat dates are *very likely* to become later, resulting in lengthening of the monsoon season. {14.2}

- The El Niño-Southern Oscillation *very likely* remains the dominant mode of interannual variability in the future in the tropical Pacific. It is *likely* that the intensity of the central Pacific warming will increase, but there is *low confidence* that the central Pacific type of El Niño will become more frequent in a warmer climate. {14.4}

- It is *likely* that both El Niño and La Niña-induced teleconnection patterns over the extra-tropical Northern Hemisphere will move eastwards in the future. {14.4}

Long-Term Projections: Ocean

- It is *very likely* that the AMOC will weaken over the 21st century with a best estimate decrease in 2100 of about 20–30% for the RCP4.5 scenario and 36–44% for the RCP8.5 scenario. It is *very unlikely* that the AMOC will undergo an abrupt transition or collapse in the 21st century, and it is *unlikely* that the AMOC will collapse beyond the 21st century for the scenarios considered. {12.5.5}

- The climate model projections suggest that regions with high sea surface salinity in the subtropics that are dominated by net evaporation will typically become more saline; regions with lower sea surface salinity at high latitudes will typically become fresher. {12.4.7, Figure 12.34}

- On multidecadal timescales, the rate of ocean heat uptake is projected to increase while the radiative forcing increases. Because the ocean integrates the surface heat flux, projections of changes in ocean heat content following different scenarios do not significantly diverge for several decades {13.4.1, 13.5.1}.

Long-Term Projections: Cryosphere

It is *very likely* that the Arctic sea ice cover will continue to shrink and thin in the course of the 21st century as global temperature rises. There is *high confidence* that an increase in annual mean global surface temperature greater than 2°C above present will eventually lead to a nearly ice-free Arctic Ocean in late summer (see Figures SPM.5 and SPM.6). {12.4.6, Figure 12.28}

- Reductions in Arctic sea ice are projected for all scenarios and year-round, with reductions in sea ice extent ranging from 39% for RCP2.6 to 94% for RCP8.5 in September and from 9% to 35% in February by the end of the century (see Figures SPM.5 and SPM.6). {12.4.6, Figure 12.28}

- For RCP8.5 it is *very likely* that the September Arctic sea ice will nearly vanish, i.e., the extent will fall below $10^6 km^2$, before the end of the century (see Figures SPM.5 and SPM.6). {12.4.6, Figure 12.28}

- There is *low confidence* in model projections of Southern Hemisphere sea ice extent for the end of the 21st century. {12.4.6, Figure 12.28}

- It is *very likely* that Northern Hemisphere snow cover will decrease as global temperatures increase. Projections of the reduction in the area of spring snow cover in the Northern Hemisphere by the end of the 21st century vary between 7% (RCP2.6) and 25% (RCP8.5). {12.4.6}

- A reduction in permafrost extent with rising global temperatures is *virtually certain*. Near-surface permafrost area is projected to decrease by between 37% (RCP2.6) and 81% (RCP8.5) by the end of the 21st century. {12.4.6}

Long-Term Projections: Sea Level

It is *very likely* that the rate of global mean sea level rise during the 21st century will exceed the rate observed during 1971–2010 for all RCP scenarios. Together, ocean thermal expansion and glaciers are *very likely* to make the largest contributions during the 21st century (see Figure SPM.7). {13.5.1, Table 13.5, Figure 13.8, Figure 13.9}

[INSERT FIGURE SPM.7 HERE]
Figure SPM.7: Projections of total global mean (top) and regional mean (bottom) sea level change from 2000 to 2100 for the two emissions scenarios RCP2.6, and RCP8.5. The total sea level change results from various contributions whose estimated ranges are given over the period 2081–2100. The scenario-dependent contributions of thermal expansion are derived from CMIP5 model simulations, glaciers and surface mass balances from the Greenland and Antarctic ice sheets are estimated from CMIP5 results using parametrised schemes based on recent studies. Contributions from ice-sheet dynamical changes and anthropogenic land water storage are also included; they are independent of scenario, and are treated as having uniform probability distributions. The maps of projected regional mean sea level change include a correction for glacial isostatic adjustment for the period 2081–2100 compared to 1986–2005. See Appendix 13.A for methods. {Figure 13.8, Figure 13.9, Figure 13.15} [PLACEHOLDER FOR SECOND ORDER DRAFT: Information on robustness and model agreement to be considered.]

- For the period 2081 to 2100, compared to 1986 to 2005, global mean sea level rise is *likely* (*medium confidence*) to be in the range 0.29–0.55 m for RCP2.6, 0.36–0.63 m for RCP4.5, 0.37–0.64 m for RCP6.0, and 0.48–0.82 m (0.56–0.96 m by 2100 with a rate of rise 8 to 15 mm yr^{-1} over the last decade of the 21st century) for RCP8.5 (see Figure SPM.7, Table SPM.2). {13.5.1, Table 13.5, Figure 13.8, Figure 13.9}

- These projections include estimates of dynamical ice loss from Greenland and Antarctica (see Figure SPM.7). However, there is *low confidence* in models of ice sheet dynamics, and there is no consensus about the reliability of semi-empirical models that give higher projections than process-based models. As a result, larger values of sea level rise cannot be excluded, but current scientific understanding is insufficient for evaluating the probability of higher values. {13.4.4, 13.5.1, Table 13.5, Figure 13.8, Figure 13.9}

- Global mean sea level rise will *very likely* continue beyond 2100, with ocean thermosteric sea level rise to continue for centuries to millennia, unless global temperatures decline. The few available model results indicate global mean sea level rise by 2300 *likely* to be less than 1 m for greenhouse gas concentrations below 500 ppm CO_2-equivalent scenario but rise as much as 1–3 m for concentrations above 700 ppm CO_2-equivalent{13.5.2, Figure 13.10, Figure 13.11}.

Long-Term Projections: Carbon and Other Biogeochemical Cycles

- It is *very likely* that the global ocean will be a net carbon sink in all RCP scenarios. It is *very likely* that global land will be a net carbon sink for scenarios with decreasing areas of anthropogenic land-use (RCP4.5, RCP6.0). For scenarios with increasing areas of land-use (RCP2.6, RCP8.5), a net land sink is *likely*, but some models project a source by 2100. {6.4, Figures 6.19–6.22, Figure 6.24}

Based on coupled carbon cycle - climate models it is *very likely* that the feedback between climate and the carbon cycle is positive in the 21st century and beyond. These models indicate a loss of carbon of 59 [20 to 98] PgC and 17 [13 to 21] PgC per °C warming from the land and the ocean, respectively. {6.4.2.1, Figure 6.20}

- For RCP2.6, large reductions in CO_2 emissions relative to present day are projected. It is about *as likely as not* that sustained globally negative emissions will be required for this scenario. {6.4, Figure 6.25, Figure 6.26}

- Anthropogenic ocean acidification, evidenced by a decrease in pH, is projected to continue worldwide over the 21st century in all RCPs (see Figure SPM.5). The largest decrease in pH is projected to occur in the warmer low and mid-latitudes. It is *likely* that surface waters in the Southern Ocean become corrosive for a less stable form of calcium carbonate by 2100, and even before in the Arctic Ocean (see Figure SPM.6). {6.4, Box 6.5, Figure 6.28}

- There is *medium confidence* on the magnitude of carbon losses through CO_2 or CH_4 emissions to the atmosphere from thawing permafrost. Projections for 2100 range from 33 to over 400 PgC for RCP8.5. {6.4.3}

Long-Term Projections: Climate Stabilization, Commitment and Irreversibility

Many aspects of climate change will persist for centuries even if concentrations of greenhouse gases are stabilised. This represents a substantial multi-century commitment created by human activities today. {12.5.4}

- Emission pathways that *likely* limit warming below 2°C above pre-industrial by 2100 indicate that CO_2-equivalent emissions cannot exceed 8.5–12.6 PgC yr^{-1} by 2020, and 4.6–6.3 PgC yr^{-1} by 2050. Median 2010 emissions are 13.1 PgC yr^{-1}. The 2°C temperature target implies cumulative carbon emissions by 2100 to be below about 1000–1300 PgC in the set of scenarios considered, of which about 545 [460 to 630] PgC were already emitted by 2011. {12.5.4}

- Continuing greenhouse gas emissions beyond 2100 as in the RCP8.5 extension induces a total radiative forcing above 12 W m^{-2} by 2300 that leads to a warming of 8.7 [5.0–11.6] °C by 2300 relative to 1986–2005. Substantial sustained reductions of emissions beyond 2100 could keep the total radiative forcing below 2 W m^{-2} by 2300, as for example in the RCP2.6 extension, which reduces the warming to 0.6 [0.3–1.0] °C by 2300. {12.3.1, 12.5.1}

- For scenarios driven by carbon dioxide alone, global average temperature is projected to remain approximately constant for many centuries following a complete cessation of emissions. Thus a large fraction of climate change is largely irreversible on human time scales, except if net anthropogenic greenhouse gas emissions were strongly negative over a sustained period. {12.5.5}

- Surface melting of the Greenland ice sheet is projected to exceed accumulation for global mean surface air temperature over 3.1 [1.9–4.6] °C above preindustrial, leading to ongoing decay of the ice sheet. The loss of the Greenland ice sheet is not inevitable, because surface melting has long time scales and it might re-grow to most of its original volume if global temperatures decline. However, a significant decay of the ice sheet may be irreversible. {13.3.3, 13.4.3, 13.4.4, Figure 13.11}

Tables

Table SPM.1: Recent trends, assessment of human influence on the trend, and projections for extreme weather and climate events for which there is an observed late-20th century trend. Bold indicates a revised assessment since AR4 (2007), (*) indicates a revised assessment from the SREX (2012) and (#) indicates that an assessment was not provided by either AR4 or SREX. {TS TFE9.1, 2.6, 11.3.2, 12.4.3, 12.4.4, 12.4.5}

Phenomenon and direction of trend	Likelihood that trend occurred in late 20th century (typically post 1950)	Likelihood of a human contribution to observed trend	Likelihood of future trends based on projections for the next few decades[#]	Likelihood of future trends based on projections for 21st century using RCP scenarios
Warmer and fewer cold days and nights over most land areas	*Very likely*	***Very likely**** [a]	*Very likely*	*Virtually certain*
Warmer and more frequent hot days and nights over most land areas	*Very likely*	***Very likely**** [a]	*Very likely*	*Virtually certain*
Warm spells/heat waves. Frequency increases over most land areas	***Medium confidence***	***Likely*** [b]	*Likely*	*Very likely*
Heavy precipitation events. Frequency (or proportion of total rainfall from heavy falls) increases over more areas than decreases	*Likely*	***Medium confidence***	*Likely*	*Very likely** [c]
Increases in frequency and/or intensity of drought[d]	*Low confidence** [d]	*Low confidence** [d]	Not assessed	*Likely* in some regions* [d]
Intense tropical cyclone activity increases	***Low confidence*** [e]	***Low confidence*** [e]	*Low confidence*	***Medium confidence***

Notes:
(a) SREX assessed *likely* anthropogenic influence on trends at the global scale.
(b) SREX did not provide an explicit attribution of warm spells/heat waves to human contributions.
(c) SREX assessed a *likely* increase in the frequency of heavy precipitation events or increase in the proportion of total rainfall from heavy falls over many areas of the globe, in particular in high latitudes and tropical regions.
(d) AR4 assessed the overall area affected by drought. SREX assessed with *medium confidence* that some regions of the world had experienced more intense and longer droughts, and *medium confidence* that anthropogenic influence had contributed to some observed changes in drought pattern. There was also *medium confidence* in a projected increase in duration and intensity of droughts in some regions of the world.
(e) Assessments of 50-year global trends limited by data uncertainties. Higher confidence of increased activity in some regions linked to anthropogenic aerosol forcing.

Table SPM.2: Projected change in global average surface air temperature (SAT) and sea level rise (SLR) for three time horizons during the 21st century. {Table 12.2, Table 13.5, 12.4.1, 11.3.2}

Variable	Scenario	2016–2035**	Level of Confidence*	2046–2065	Level of Confidence*	2081–2100	Level of Confidence*
ΔSAT[a] [°C]	RCP2.6	0.7 [n/a]	n/a	1.0 [n/a]	n/a	1.0 [0.2–1.8]	*high*
	RCP4.5	0.7 [n/a]	n/a	1.4 [n/a]	n/a	1.8 [1.0–2.6]	*high*
	RCP6.0	0.7 [n/a]	n/a	1.3 [n/a]	n/a	2.3 [1.3–3.2]	*high*
	RCP8.5	0.8 [n/a]	n/a	2.0 [n/a]	n/a	3.7 [2.6–4.8]	*high*
Total SLR[b] [m]	RCP2.6	0.11 [0.08–0.14]	*medium*	0.25 [0.19–0.33]	*medium*	0.42 [0.29–0.55]	*medium*
	RCP4.5	0.11 [0.08–0.14]	*medium*	0.27 [0.20–0.35]	*medium*	0.49 [0.36–0.63]	*medium*
	RCP6.0	0.11 [0.07–0.14]	*medium*	0.26 [0.19–0.34]	*medium*	0.50 [0.37–0.64]	*medium*
	RCP8.5	0.12 [0.08–0.15]	*medium*	0.31 [0.23–0.39]	*medium*	0.64 [0.48–0.82]	*medium*

Notes:
(a) CMIP5 ensemble; anomalies calculated with respect to 1986–2005; Numbers are in the format: mean [likely range]
(b) 21 CMIP5 models; anomalies calculated with respect to 1986–2005. Where CMIP5 results were not available for a particular AOGCM and scenario, they were estimated as explained in Chapter 13, Table 13.5. The contributions from ice sheet dynamical change and anthropogenic land water storage are treated as independent of scenario, since scenario dependence cannot be evaluated on the basis of existing literature, and as having uniform probability distributions, uncorrelated with the magnitude of global climate change. Numbers are in the format: mean [likely range]
* [PLACEHOLDER FOR SECOND ORDER DRAFT: Level of confidence to be updated]
** [PLACEHOLDER FOR SECOND ORDER DRAFT: Near-term values and ranges to be updated]

Figures

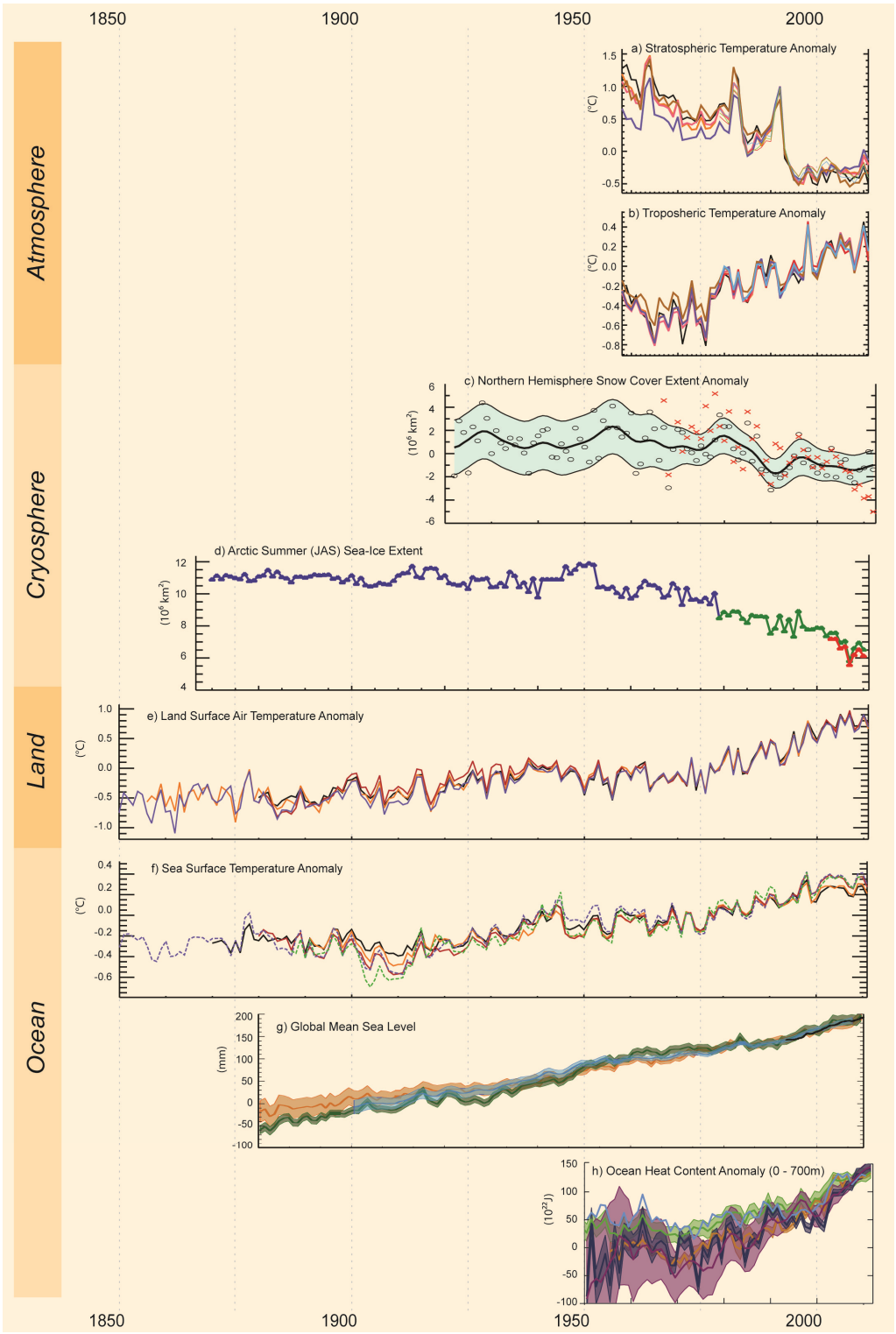

Figure SPM.1: Multiple observed indicators of a changing global climate. Each line represents an independently derived estimate of change in various large-scale quantities from the atmosphere, the cryosphere, the land, and the ocean. In panels where individual datasets overlap, the datasets have been normalized to a common period of record. Anomalies are relative to the mean of 1981–2000 (panels a and b), 1971–2000 (panel c), 1961–1990 (panels e and f), and the year 1971 (panel h). Panel c provides the 13-year running mean of the March-April Snow Cover Extent (SCE) anomaly for the full observational record, and June SCE (x's) for the satellite period only. Full details of the datasets shown here are provided in the Supplementary Material to Chapters 2 and Chapter 4. Where available, uncertainties in the observations are indicated by a shaded range. {Figure 2.15, Figure 2.19, Figure 2.24, Figure 3.2, Figure 3.13, Figure 4.3, Figure 4.19}.

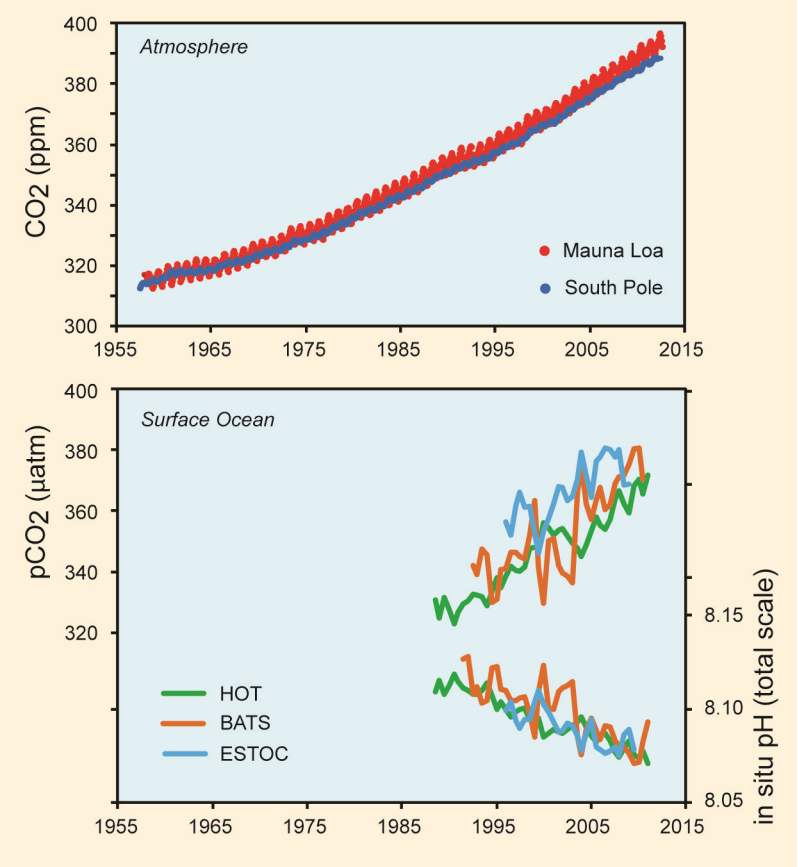

Figure SPM.2: Multiple observed indicators of a changing global carbon cycle. Measurements of atmospheric concentrations of carbon dioxide (CO_2) are from Mauna Loa and South Pole since 1958. Measurements of partial pressure of CO_2 at the ocean surface are shown from three stations from the Atlantic and the Pacific Oceans, along with the measurement of in situ pH, a measure of the acidity of ocean water. These stations are the Hawaii Ocean Time-series (HOT) from the station ALOHA, the Bermuda Atlantic Time-series Study (BATS), and the European Station for Time series in the Ocean (ESTOC). Full details of the datasets shown here are provided in the underlying report. {Figure 2.1, Figure 3.17}.

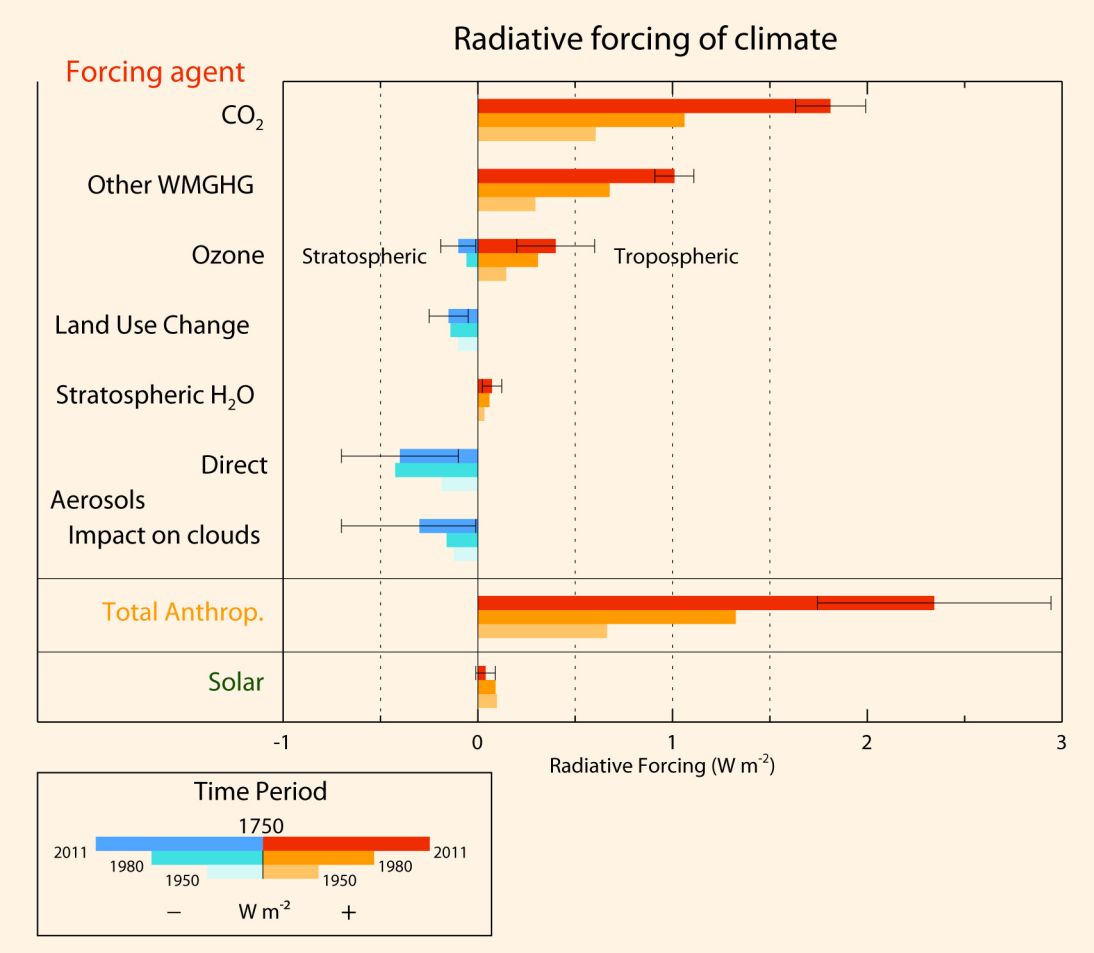

Figure SPM.3: Global average radiative forcing (RF) estimates and ranges for various drivers and three successive time periods; 1750–1950, 1750–1980, 1750–2011. The anthropogenic drivers are carbon dioxide (CO_2), other well-mixed greenhouse gases (CH_4, N_2O, and others), ozone, land use change, statospheric water vapour, and aerosols, with the sum of all contributions indicated. Assessed uncertainty ranges are given by black intervals. The RF of solar irradiance, a natural driver, is also estimated for the three time periods. {Figure 8.17}

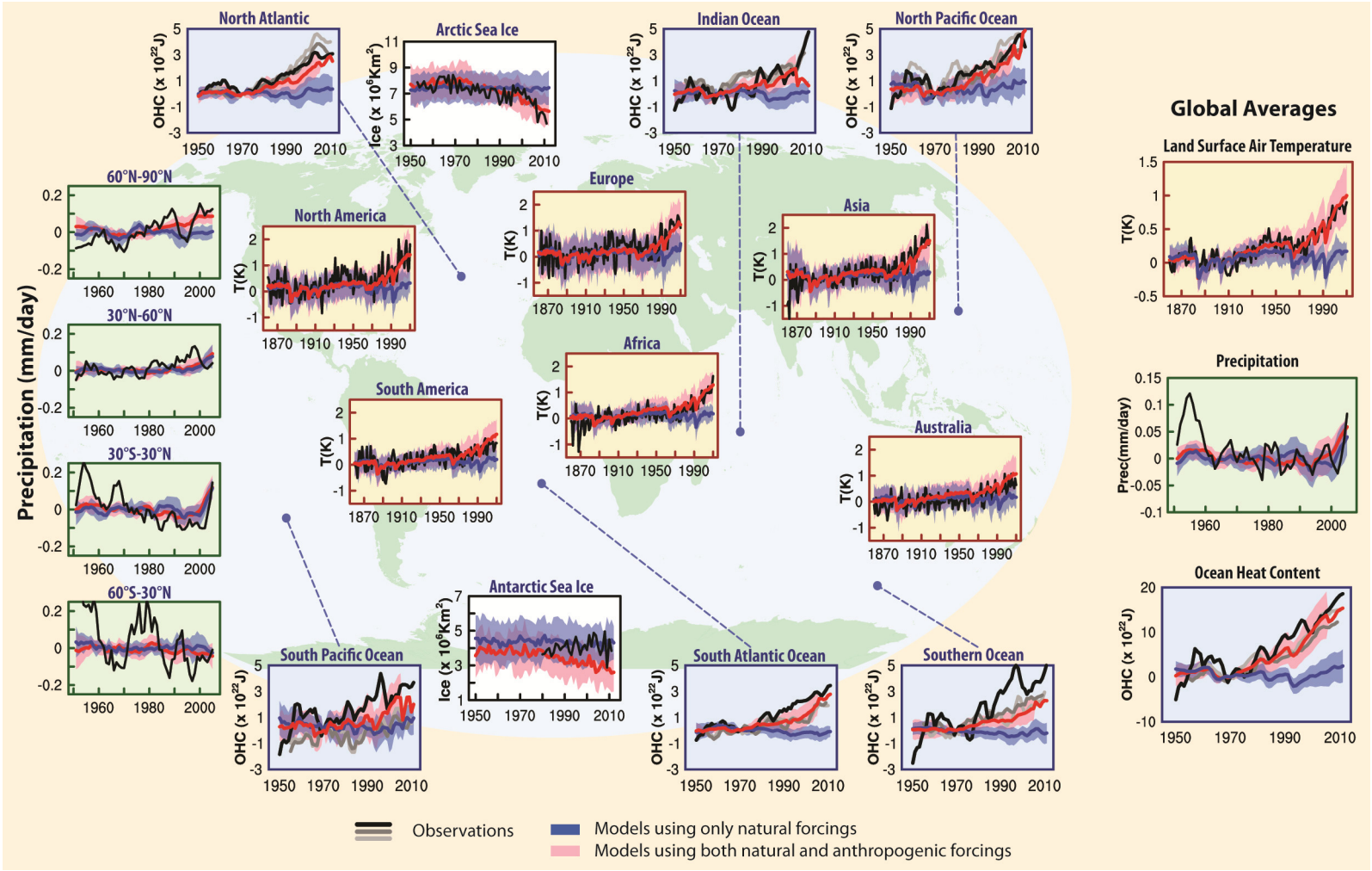

Figure SPM.4: Comparison of observed and simulated climate change based on four large-scale indicators in the atmosphere, cryosphere and the ocean. Indicators are time series of continental land surface air temperatures (1850–2010, yellow padded panels), zonal mean precipitation in latitude bands (1950–2010, green padded panels), Arctic and Antarctic sea ice (1950–2010, white padded panels), and ocean heat uptake in the major ocean basins (1950–2010, blue padded panels). Global mean changes are also given. In all panels, black/grey curves indicate observation-based estimates, blue curves and bands are multi-model mean and ensemble ranges based on simulations forced by natural drivers only, and red curves and bands are for simulations forced by natural and anthropogenic drivers. The bands indicate the 5 to 95% for temperature, and one standard deviation for precipitation, sea ice, and ocean heat content. Model results are based on the ensemble of CMIP5. For sea ice extent the seven CMIP5 models are considered that matched the mean minimum and seasonality with less than 20% error compared with observations. Full details are provided in the Appendix of Chapter 10. {Figure 10.15, 10.20}

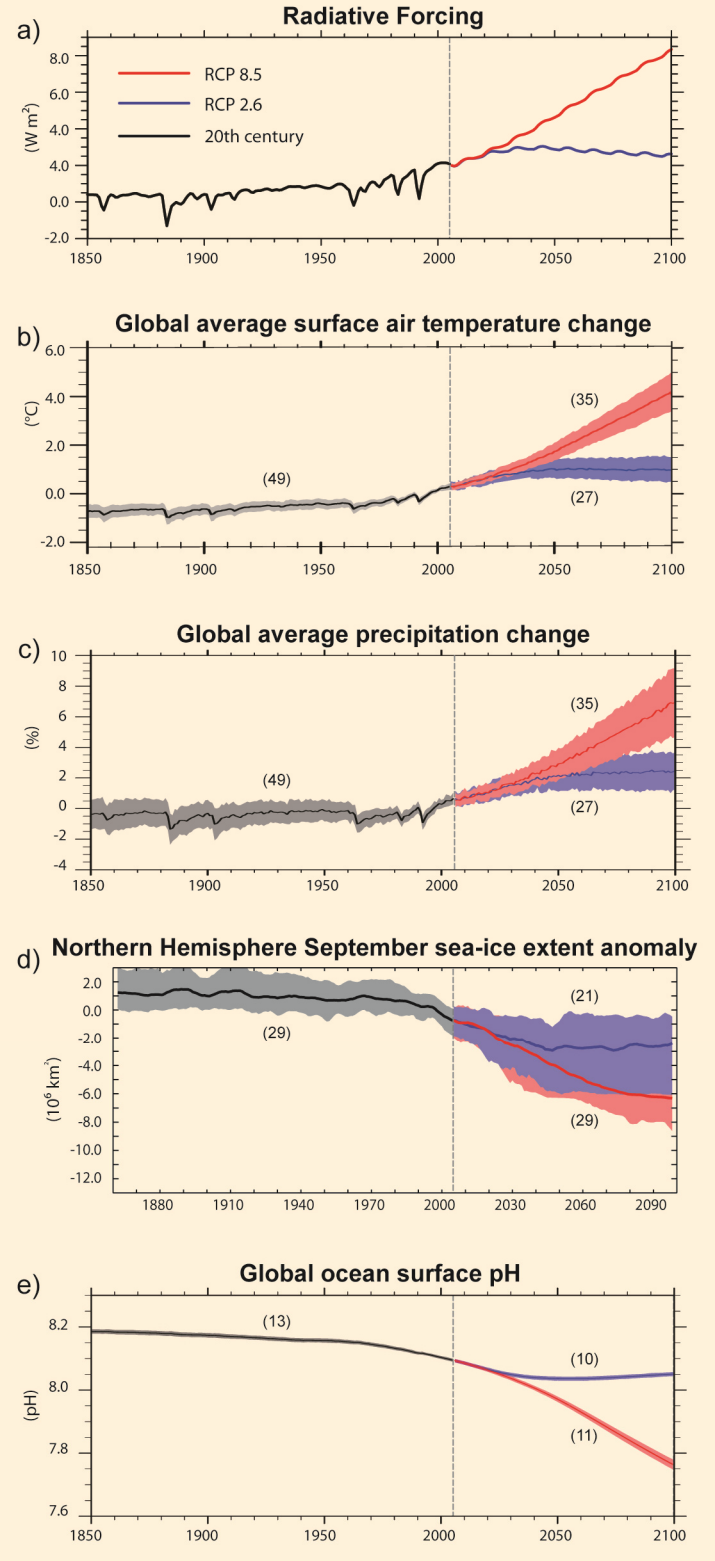

Figure SPM.5: CMIP5 multi-model simulated time series. Panel (a) provides the radiative forcing reconstructed for the historical time period and projected for the future. Other panels provide mean changes (relative to 1986–2005) of (b), global annual mean surface air temperature, (c), global annual mean precipitation, (d), Northern Hemisphere sea-ice extent anomaly in September, and (e), global mean ocean surface pH from CMIP5 climate model simulations from 1850 to 2100. Projections are shown for emissions scenarios RCP2.6 (blue) and RCP8.5 (red) for the multi-model mean (solid lines) and ±1 standard deviation across the distribution of individual model simulations (shading). Black (grey shading) is the modelled historical evolution using historical reconstructed forcings. For pH, a subset of the CMIP5 models is chosen which simulate the global carbon cycle and which are driven by prescribed atmospheric CO_2 concentrations. The number of CMIP5 models to calculate the multi-model mean is indicated for each time period/scenario. {Figure 12.5, Figure 12.28, Figure 6.28}

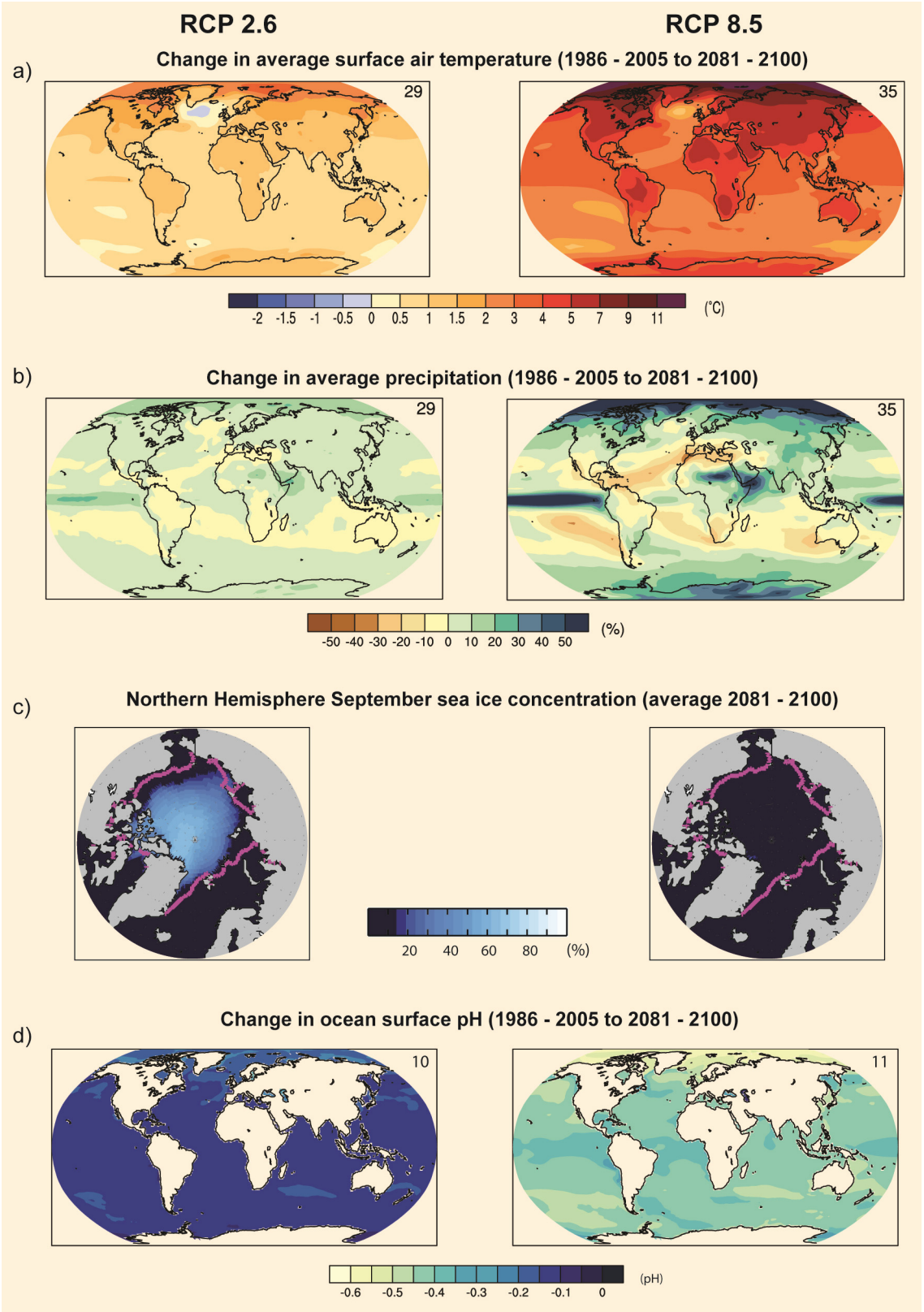

Figure SPM.6: Maps of multi-model results in 2081–2100 (relative to 1986–2005) of (a), surface air temperature change, (b), average percent change in mean precipitation, (c), Northern Hemisphere sea ice concentration, and (d) change in global ocean surface pH. The two emissions scenarios RCP2.6, and RCP8.5 are considered. The number of CMIP5 models to calculate the multi-model mean is indicated in the upper right corner of each panel. The pink lines in panels (c) show the observed 15% sea ice concentration limits averaged over 1986–2005 for comparison. {Figure 12.11, Figure 12.22, Figure 12.29, Figure 6.28}. [PLACEDHOLDER FOR SECOND ORDER DRAFT: Information on robustness and model agreement to be considered.]

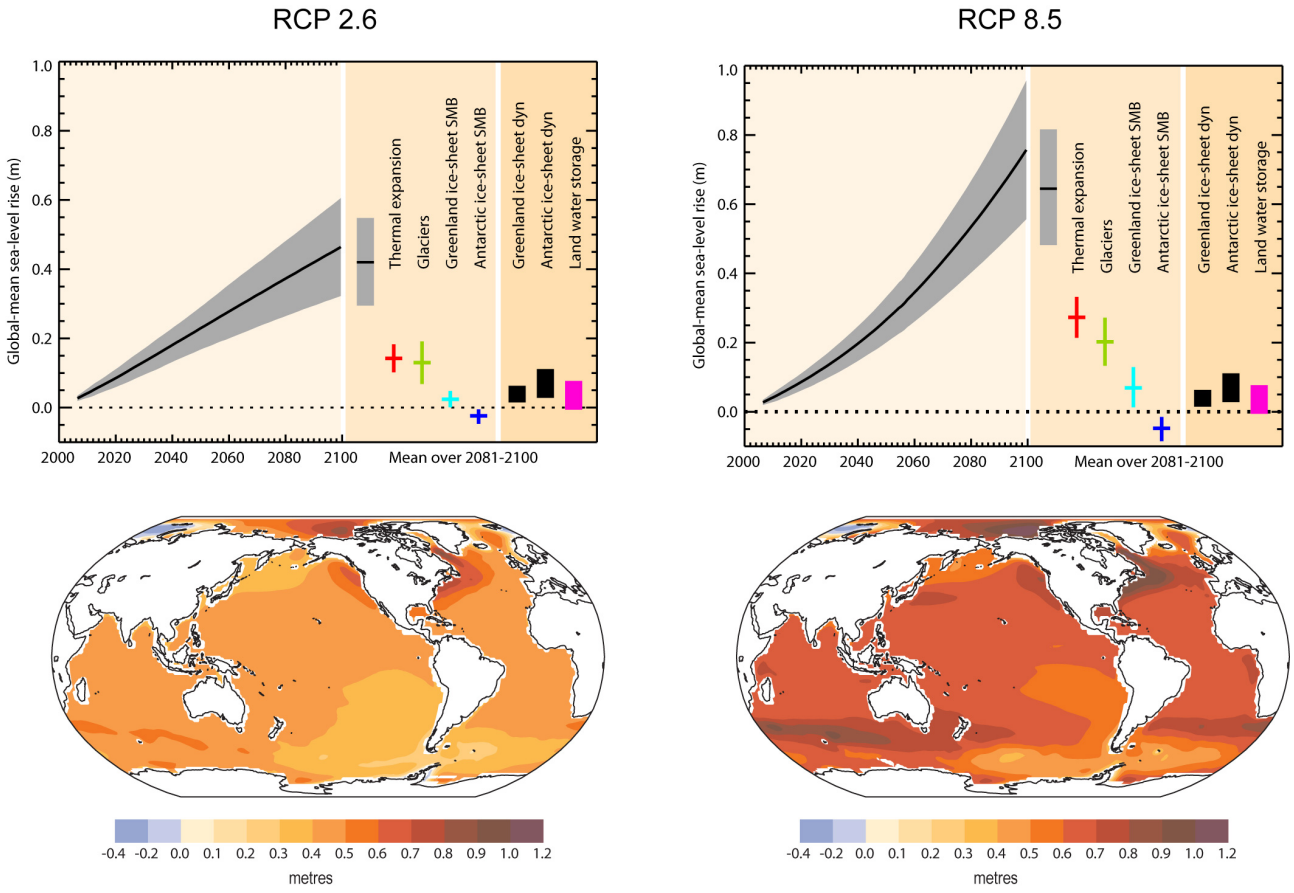

Figure SPM.7: Projections of total global mean (top) and regional mean (bottom) sea level change from 2000 to 2100 for the two emissions scenarios RCP2.6, and RCP8.5. The total sea level change results from various contributions whose estimated ranges are given over the period 2081–2100. The scenario-dependent contributions of thermal expansion are derived from CMIP5 model simulations, glaciers and surface mass balances from the Greenland and Antarctic ice sheets are estimated from CMIP5 results using parametrised schemes based on recent studies. Contributions from ice-sheet dynamical changes and anthropogenic land water storage are also included; they are independent of scenario, and are treated as having uniform probability distributions. The maps of projected regional mean sea level change include a correction for glacial isostatic adjustment for the period 2081–2100 compared to 1986–2005. See Appendix 13.A for methods. {Figure 13.8, Figure 13.9, Figure 13.15} [PLACEHOLDER FOR SECOND ORDER DRAFT: Information on robustness and model agreement to be considered.]